

Acoustical stability of a sonoluminescing bubble

Joachim Holzfuss and Matthias Rüggeberg

Institut für Angewandte Physik, Technische Universität Darmstadt, Schloßgartenstraße 7, 64289 Darmstadt, Germany

R. Glynn Holt

Department of Aerospace and Mechanical Engineering, Boston University, Boston, Massachusetts 02215

(Received 22 December 2000; revised manuscript received 28 June 2002; published 30 October 2002)

In the parameter region for sonoluminescence of a single levitated bubble in a water-filled resonator it is observed that the bubble may have an enormous spatial stability leaving it “pinned” in the fluid and allowing it to emit light pulses of picosecond accuracy. We report here observations of a complex harmonic structure in the acoustic field surrounding a sonoluminescing bubble. We show that this complex sound field determines the position of the bubble and may either increase or decrease its spatial stability. The acoustic environment of the bubble is the result of the excitation of high-order normal modes of the resonator by the outgoing shock wave generated by the bubble collapse.

DOI: 10.1103/PhysRevE.66.046630

PACS number(s): 43.25.+y, 78.60.Mq

The phenomenon of single-bubble sonoluminescence (SBSL) describes a bubble oscillating violently in response to a driving ultra sound field and emitting ultra short light pulses at collapse time [1,2]. This process is an elegant way to turn acoustic energy into photons and has stimulated attempts to further increase the energy concentration. However, SBSL has been shown to exist only in a small experimentally accessible region in parameter space [3]. Several stability criteria limit the SBSL region. Among these are two hydrodynamic instabilities, namely the shape or Faraday instability [4] and the Rayleigh-Taylor instability. They define boundaries in parameter space where bubbles can be driven [5]. Within this region the bubble also has to be in stable diffusional equilibrium with the gas content of the surrounding liquid. Experiments [3,6] show that in the case of air bubbles in water only argon contributes to the diffusional stability on a slow time scale. They are backed by a thesis [7] stating that chemical processes within the bubble play a role, generating fast dissolving reaction products from chemically noninert constituents. Our work focuses on the spatial stability of a sonoluminescing bubble. We have been motivated by the observation that a bubble can make discrete spatial jumps and oscillations in certain situations [8–10] and otherwise is spatially stable while maintaining volume oscillations of 6 orders of magnitude. Most researchers reported pulse to pulse jitter even under otherwise stable conditions that e.g., complicate pulse width measurements [2]. Also, several researchers surprisingly noted discrepancies between measured and predicted position of the levitated bubble [11] that were as large as 10 mm [12], or bubbles moving away from the antinode with increased driving [13]. Besides not being understood, the discrepancies leads to differences between experimental and numerical predictions of bubble dynamics and stability.

Levitating a bubble is possible because of the primary Bjerknes force

$$F_B = -\langle V(t) \nabla P_a(r, z, t) \rangle_t, \quad (1)$$

acting on the oscillating volume $V(t)$ of the bubble. When F_B is large enough to overcome the buoyancy force, the

bubble is attracted to a fixed position in the fluid. The sound pressure $P_a(r, z, t)$ is a standing wave with cylindrical coordinates r, z . At moderate driving with frequencies below their linear resonance, bubbles are attracted towards the pressure antinode to a position slightly above the pressure antinode, at which the buoyant and the Bjerknes force balance.

In the experiments a cuvette consisting of two hollow piezoceramic cylinders connected by a hollow glass tube is utilized [8,10]. The bottom is sealed with an optical glass window, the upper end remains open. The piezo ceramics are driven by an alternating voltage setting up a standing wave of 23.5 kHz. In order to record the acoustic environment of the bubble a needle hydrophone [14] is gently put within a few millimeters distance to the bubble with the help of a video camera. A translation table connected to a computer controlled stepper motor moves the hydrophone vertically upwards with step sizes of 75 μm . After each step the power lines of the motor are shut off to facilitate a noise free measurement. 60 000 data points are recorded with a sampling frequency of 10 MHz, 12 bit resolution and transferred to a workstation. Each measurement is triggered by a pulse from the driving wave form generator. 100 measurement cycles are made. Each cycle consists of positioning, digitizing and data transfer and lasts about 4 s. The overall measurement time is small to keep the partial pressure and the temperature of the water constant.

A typical measured acoustical signal taken at a fixed point near a sonoluminescing bubble driven near the upper stable SBSL threshold is shown in Fig. 1(a). It is characterized by a superposition of the driving wave, a pressure spike of the shock wave emitted by the bubble at collapse [8,15] and a higher-frequency background signal [9,10,16,17]. This signal’s amplitude is connected with the magnitude of the pressure spike. The background can have an amplitude of approximately 20% of the externally applied driving. It seems to be obvious that such a large deviation from a pure sine wave has an impact on the bubble, but so far its origin has received little attention. A striking observation is that the noisy looking signal is periodic with the driving frequency, so it is not a stochastic noise. The signal changes smoothly,

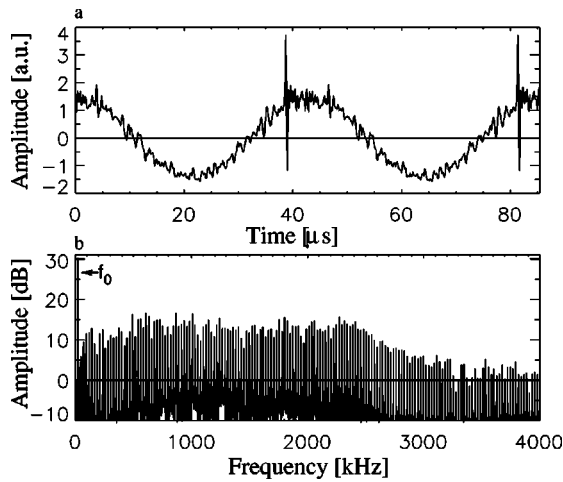


FIG. 1. Hydrophone signal 3 mm above a sonoluminescing bubble. (b) Amplitude spectrum of the peak-masked signal.

however, when the hydrophone is moved to a different location, where it looks different than before but is periodic again. The background signal appears at the lower SBSL threshold and increases in amplitude with increased driving. Above the upper threshold it disappears as does the bubble. With no bubble present, there is no background harmonic signal at any driving amplitude in the SBSL range [9,10].

Fourier transforms have been calculated in order to analyze the frequency spectrum of the signal [Fig. 1(b)]. Each measurement is sized in length to an integer multiple of the driving period to avoid windowing. The individual spectra consist of a rich harmonic spectrum extending up to 4 MHz. The amplitudes of the harmonics of the driving wave up to 2.5 MHz have large amplitudes of 20 dB below that of the driving. It is essential to note that these harmonics are not due to artifacts induced by the delta like pressure peak. These pulse peaks and eventually present high-frequency ringing have been masked in this and the subsequent analysis. Certain frequencies that are not harmonics of the driving have also been detected corresponding to the mechanical resonances of the needle hydrophone. Because their amplitudes are below the 0 dB line they are insignificant. The amplitude and the temporal phase of each harmonic are extracted from the spectrum and shown as a function of hydrophone position. The phase values are relative to cosine functions and the beginning of the time series, which is locked to the driving. Figure 2 shows a typical mode structure of the 12th harmonic of the driving frequency within the resonator: The amplitude curve shows nodes and antinodes with the appropriate 180 deg phase shifts, as seen in the phase curve of Fig. 2. Within the antinodes the temporal phases stay almost constant up to the next node.

This behavior of the harmonics extends up to very high frequencies, as seen in Fig. 3, where a mode with the frequency of the 56th harmonic is shown. A 90 deg phase shift is often observed as well (Fig. 3 at 7.3 mm). This may be explained by the superposition of modes extending in the horizontal and vertical directions. It should be noted that some harmonics do not show signs of a standing wave everywhere. Phase values continuously growing with position

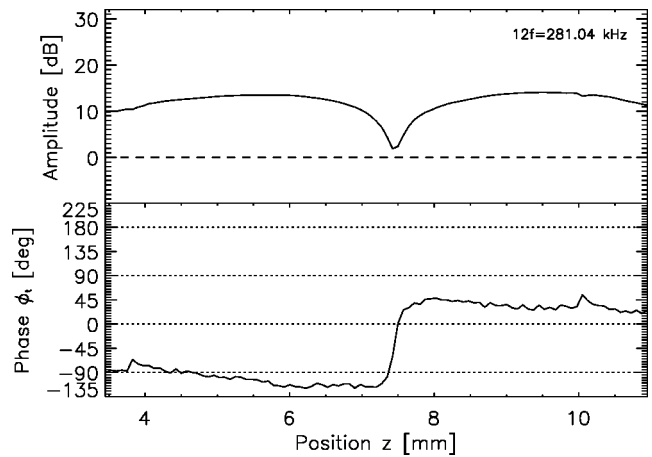


FIG. 2. Maximum amplitudes and temporal phases of sound pressure of the 12th harmonic as a function of hydrophone position relative to some point in the resonator.

are sometimes measured. They are explained by traveling wave components of the shock being reflected by the walls of the container.

The measured high-frequency standing wave behavior originates from the excitation of higher-order modes and modes of higher frequency of the cylindrical resonator. Their detection is independent on the hydrophone used [14] but depends on the special type of resonator and wall reflectivity. They are excited by high pressure pulses of the bubble-emitted shockwaves [8] in the liquid in the resonator. From the many possible modes only those with frequencies of multiples of the driving are excited. It has been shown that artificially adding a second harmonic to the driving frequency has a great impact on bubble dynamics [18,19]. It seems obvious that a measured rich harmonic structure of a sound field produced by the bubble itself has an effect on its dynamics in turn.

In order to determine these effects a numerical bubble model [8,10,20] has been integrated while a sound field $p_a(z,t)$ [Eq. 2] consisting of the first ten harmonics with the

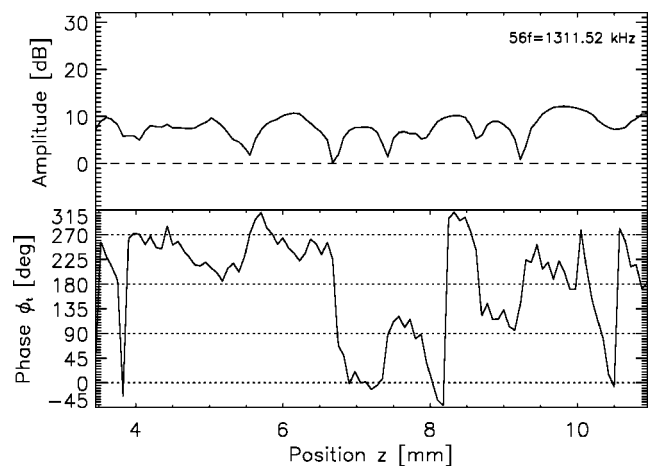


FIG. 3. Maximum amplitudes and temporal phases of sound pressure of the 56th harmonic as a function of relative hydrophone position.

TABLE I. Measured parameters for numerical calculation of a 10 frequency self-excitation [Eq. (2)]. Frequencies $\omega_i/2\pi$, amplitudes $p_{a,i}$, and spatial and temporal phases $\phi_{z,i}$ and $\phi_{t,i}$ of the harmonics have been determined by Fourier transform of the data of Fig. 1. Spatial phases are relative to $z=3.45$ mm. The right column shows the calculated individual Bjerknes forces $F_{B,i}$ on a bubble of $5 \mu\text{m}$ equilibrium radius.

i	$\omega_i/2\pi$ (kHz)	$p_{a,i}$ (mbar)	$\phi_{z,i}$ (deg)	$\phi_{t,i}$ (deg)	$F_{B,i}$ (nN)
1	23.42	1450	5.7	320	16.82
2	46.84	4	22.7	340	-0.49
3	70.26	11	-25.5	0	8.54
4	93.68	23	34.1	330	-0.17
5	117.10	26	-35.5	290	-7.39
6	140.52	38	59.7	290	-11.72
7	163.94	40	159.2	180	-0.60
8	187.36	24	-125.1	185	-0.28
9	210.78	25	25.6	270	-4.32
10	234.20	30	-127.9	90	-1.99
Buoyancy					2.03

appropriate measured parameters (Table I) is driving it. According to the measurements the vertical components of the sound field can be expressed by the sum of excited modes approximated by standing waves,

$$p_a(z,t) = \sum_{i=1}^{10} [p_{a,i} \cos(k_i z + \phi_{z,i}) \cos(\omega_i t + \phi_{t,i})], \quad (2)$$

with wave numbers $k_i = 2\pi/\lambda_i$ and λ_i the wavelengths.

Gradients $\nabla p_{a,i}(z,t)$ are used to calculate the individual Bjerknes forces by Eq. (1). The contributions of the harmonics to these forces differ (Table I, right column): positive values denote an upward pointing force (same direction as buoyancy), negative ones a downward pointing one. Interestingly, their order of magnitude is not very different. E.g., the contribution of the 6th harmonic almost has the same size as the one of the applied wave, but opposite sign. For a spatially static bubble the sum of all forces (including time averaged buoyancy) is zero. This leaves -0.43 nN for the sum of forces of not included harmonics.

Figure 4 shows the force acting on the bubble. The zero crossings denote the stable position. The difference between single wave driving (dashed line) and driving including all harmonics up to the 10th results in a spatial vertical difference of 1 mm (roughly 100 bubble radii for a bright SBSL bubble), such that the bubble actually levitates below the computed equilibrium position of single wave driving. The results show that frequency, amplitude and phase together are important for the resulting force. The time averaged buoyancy force, which is always included in the above calculations, is quite small, omitting it would shift the stable position downwards by only 0.1 mm. Also shown are the gradients of the forces. The larger absolute value in the case of the experimental full driving indicates an increase in stability through stronger bubble confinement by larger force increase. The obvious asymmetry will result in a preferred

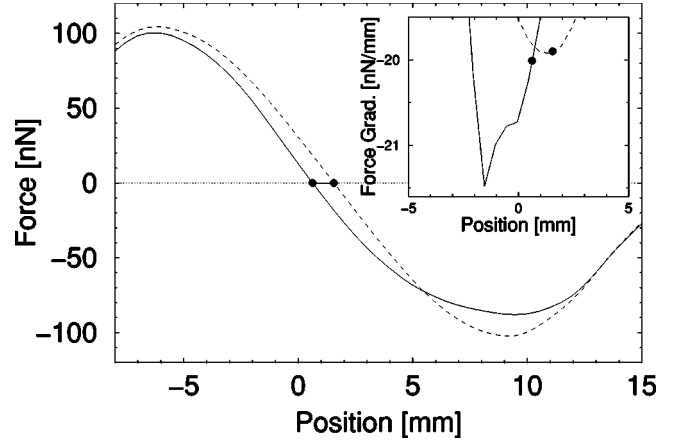


FIG. 4. Calculated force acting on a bubble (inset: gradient of the force) from measured parameters as a function of vertical distance: dashed, applied wave + buoyancy; straight, first 10 harmonics + buoyancy; stable bubble positions are marked with filled circles.

direction of spatial jitters once the bubble gets unstable. That the bubble is not oscillating in the extremum of the force gradient may be seen as a sign of an upcoming instability upon further increase of the driving.

It is clear that the typical SBSL bubble creates its own acoustic environment, within which it is often highly (spatially) stable. But stability is not always achieved. Spatial oscillations have been observed (Fig. 5) that can be explained as follows: The bubble is setting up a standing wave field by pumping energy into higher harmonic modes.

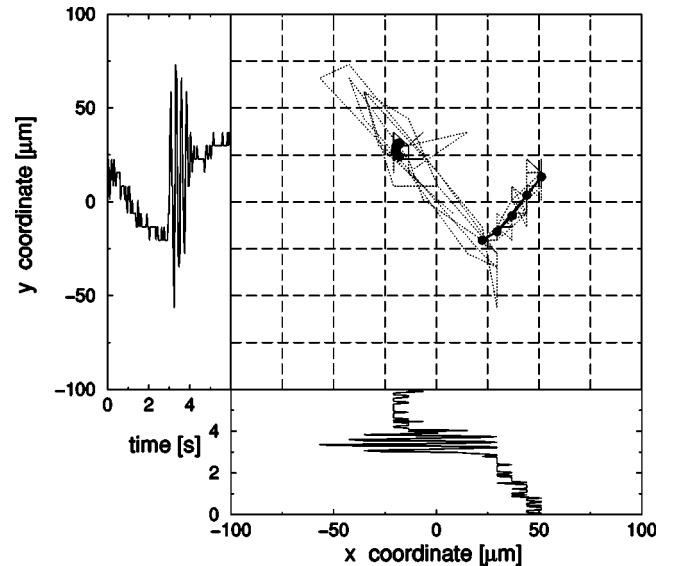


FIG. 5. Horizontal positions of a sonoluminescing bubble during diffusive growth. Dotted lines show actual positions; thick lines and dots are fits to the traces before and after the spatial oscillations. Starting on the right side the bubble moves along the line and jumps back and forth several times to its later end point. The side plots are time traces of projections of the bubble onto the horizontal xy plane, which have been recorded by photographing shock wave emissions [8].

Through feedback the bubble is moved in space by the resulting Bjerknes forces. At the new location either the applied driving is different (resulting in a change in dynamics) or certain modes cannot be excited well. Because of that the bubble is forced back to the old position and things start over again. The discreteness of the positions can be well understood in light of the standing wave patterns reported here. This scenario will manifest itself most dramatically when parameters change (e.g., if the bubble is diffusively unstable such that the equilibrium radius changes). Numerical calculations show, that very high harmonics with the above measured amplitudes do not directly change the dynamics of the bubble. They have a strong impact on bubble position and can indirectly change the dynamics by moving it to positions with another driving amplitude.

We have shown that the strong acoustic harmonic background in sonoluminescence experiments has its origin in the

bubble dynamics themselves. A shock wave emitted by the bubble into the fluid in interaction with the resonator generates a complex mode field with a fine structure consisting of contributions from higher harmonics of the applied driving. The spatial modes have been shown to be responsible for the positioning of a bubble and for the spatial stability it experiences. Higher harmonic modes together with ballistic effects of the shock wave may result in an acoustic instability and play an important role in the determination of limits of parameter ranges of stable sonoluminescence. Knowing and controlling this instability may lead to a reduction of pulse jitter to e.g., facilitate Hanbury-Brown and Twiss experiments. When comparing numerical and experimental bubble dynamics (after-ringing) the background signal should be considered.

The authors thank R.A. Roy and W. Seelig for stimulating discussions. The work has been funded by SFB 185 "Nicht-lineare Dynamik" of the DFG.

-
- [1] D.F. Gaitan, L.A. Crum, C.C. Church, and R.A. Roy, *J. Acoust. Soc. Am.* **91**, 3166 (1992); B.P. Barber and S.J. Putterman, *Nature (London)* **352**, 318 (1991); B.P. Barber, R.A. Hiller, R. Löfstedt, S.J. Putterman, and K.R. Weninger, *Phys. Rep.* **281**, 65 (1997).
 - [2] R. Pecha, B. Gompf, G. Nick, Z.Q. Wang, and W. Eisenmenger, *Phys. Rev. Lett.* **81**, 717 (1998).
 - [3] R.G. Holt and D.F. Gaitan, *Phys. Rev. Lett.* **77**, 3791 (1996).
 - [4] R. G. Holt, J. Holzfuss, A. Judt, A. Phillip, and S. Horsburgh, in *Frontiers of Nonlinear Acoustics: Proceedings of the 12th ISNA*, edited by M. F. Hamilton and D. T. Blackstock (Elsevier Science, London, 1990), pp. 497–502.
 - [5] D.F. Gaitan and R.G. Holt, *Phys. Rev. E* **59**, 5495 (1999); R. G. Holt and D. F. Gaitan, in *Proceedings of the 3rd Microgravity Fluid Physics Conference, Cleveland, OH* (NASA, Washington, DC, 1996), Vol. 3338, p. 591.
 - [6] B.P. Barber, K. Weninger, R. Löfstedt, and S. Putterman, *Phys. Rev. Lett.* **74**, 5276 (1995); J.A. Ketterling and R.E. Apfel, *ibid.* **81**, 4991 (1998); T.J. Matula and L.A. Crum, *ibid.* **80**, 865 (1998).
 - [7] D. Lohse, M.P. Brenner, T.F. Dupont, S. Hilgenfeldt, and B. Johnston, *Phys. Rev. Lett.* **78**, 1359 (1997).
 - [8] J. Holzfuss, M. Rüggeberg, and A. Billo, *Phys. Rev. Lett.* **81**, 5434 (1998).
 - [9] M. Rüggeberg, J. Holzfuss, and R.G. Holt, *J. Acoust. Soc. Am.* **104**, 1771 (1998).
 - [10] M. Rüggeberg, *Stosswellenemission und die Akustische Umgebung einer Sonolumineszierenden Blase* (Shaker, Aachen, 2000).
 - [11] T.J. Matula, S.M. Cordry, R.A. Roy, and L.A. Crum, *J. Acoust. Soc. Am.* **102**, 1522 (1997).
 - [12] R.A. Hiller, S.J. Putterman, and K.R. Weninger, *Phys. Rev. Lett.* **80**, 1090 (1998).
 - [13] K. Weninger, R. Hiller, B.P. Barber, D. Lacoste, and S.J. Putterman, *J. Phys. Chem.* **99**, 14 195 (1995).
 - [14] Dapco Industries, NP10-3, diameter 1.3 mm, length 78 mm, linearity 3db (1–10 MHz); for comparison and calibration have been used: Precision Acoustics Ltd. HPM05/2, diameter 0.5 mm, length 3 in, linearity 4 db (1–15 MHz), Reson A/S TC4013, linearity 3 db (5–110 kHz).
 - [15] T.J. Matula, I.M. Hallaj, R.O. Cleveland, L.A. Crum, W.C. Moss, and R.A. Roy, *J. Acoust. Soc. Am.* **103**, 1377 (1998).
 - [16] F.B. Seeley, *J. Acoust. Soc. Am.* **105**, 2236 (1999).
 - [17] See, e. g., Figs. 1 and 2 in K.R. Weninger, B.P. Barber, and S.J. Putterman, *Phys. Rev. Lett.* **78**, 1799 (1997).
 - [18] J. Holzfuss, M. Rüggeberg, and R. Mettin, *Phys. Rev. Lett.* **81**, 1961 (1998).
 - [19] F.J. Moraga, R.P. Taleyarkhan, R.T. Lahey, and F.J. Bonetto, *Phys. Rev. E* **62**, 2233 (2000).
 - [20] F. R. Gilmore, Hydrodynamics Laboratory California Institute of Technology (Pasadena), Report No. 26-4, 1952 (unpublished).